HHS Public Access

Author manuscript

J Matern Fetal Neonatal Med. Author manuscript; available in PMC 2017 October 03.

Published in final edited form as:

J Matern Fetal Neonatal Med. 2016 ; 29(7): 1046–1054. doi:10.3109/14767058.2015.1038518.

Placenta-on-a-Chip: A novel platform to study the biology of the human placenta

Ji Soo Lee, B.Eng[1], **Roberto Romero, MD, D.Med.Sci**[2,3,4,5], **Yu Mi Han, PhD**[6], **Hee Chan Kim, PhD**[7,8,9], **Chong Jai Kim, MD**[10], **Joon-Seok Hong, MD**[6], and **Dongeun Huh, PhD**[11]

[1]Interdisciplinary Program of Bioengineering, Seoul National University Graduate School, Seoul, Republic of Korea

[2]Perinatology Research Branch, Program for Perinatal Research and Obstetrics, Division of Intramural Research, Eunice Kennedy Shriver National Institute of Child Health and Human Development, NIH, Bethesda, MD and Detroit, MI

[3]Department of Obstetrics and Gynecology, University of Michigan, Ann Arbor, MI

[4]Department of Epidemiology and Biostatistics, Michigan State University, East Lansing, MI

[5]Department of Molecular Obstetrics and Genetics, Wayne State University, Detroit, MI

[6]Department of Obstetrics and Gynecology, Seoul National University Bundang Hospital, Bundang, Republic of Korea

[7]Institute of Medical and Biological Engineering, Medical Research Center, Seoul National University, Seoul, Republic of Korea

[8]Department of Biomedical Engineering, Seoul National University College of Medicine, Seoul, Republic of Korea

[9]Department of Biomedical Engineering Seoul National University Hospital, Seoul, Republic of Korea

[10]Department of Pathology, Asan Medical Center, University of Ulsan College of Medicine, Seoul, Republic of Korea

[11]Department of Bioengineering, University of Pennsylvania, Philadelphia, PA

Abstract

Objective—Studying the biology of the human placenta represents a major experimental challenge. Although conventional cell culture techniques have been used to study different types of placenta-derived cells, current *in vitro* models have limitations in recapitulating organ-specific

Correspondence: Dongeun Huh, PhD, Department of Bioengineering, University of Pennsylvania, 240 Skirkanich Hall, 210 S. 33rd Street, Philadelphia, PA 19104, USA, Telephone: (215) 898-5208, huhd@seas.upenn.edu, Joon-Seok Hong, MD. PhD, Department of Obstetrics and Gynecology, Seoul National University Bundang Hospital, 82, Gumi-ro 173 beon-gil, Bundang-gu, Seongnam-si, Gyeonggi-do, 463-707, Republic of Korea, Telephone: 82-31-787-7256, FAX: 82-31-787-4054, hjsobgy@gmail.com, Roberto Romero, MD, D. Med. Sci, Perinatology Research Branch, NICHD/NIH/DHHS, Wayne State University/Hutzel Women's Hospital, 3990 John R, Box 4, Detroit, MI 48201, USA, Telephone: (313) 993-2700, Fax: (313) 993-2694, romeror@mail.nih.gov.

Declaration of Interest

The authors report no conflicts of interest.

structure and key physiological functions of the placenta. Here we demonstrate that it is possible to leverage microfluidic and microfabrication technologies to develop a microengineered biomimetic model that replicates the architecture and function of the placenta.

Materials and methods—A "Placenta-on-a-Chip" microdevice was created by using a set of soft elastomer-based microfabrication techniques known as soft lithography. This microsystem consisted of two polydimethylsiloxane (PDMS) microfluidic channels separated by a thin extracellular matrix (ECM) membrane. To reproduce the placental barrier in this model, human trophoblasts (JEG-3) and human umbilical vein endothelial cells (HUVECs) were seeded onto the opposite sides of the ECM membrane and cultured under dynamic flow conditions to form confluent epithelial and endothelial layers in close apposition. We tested the physiological function of the microengineered placental barrier by measuring glucose transport across the trophoblast-endothelial interface over time. The permeability of the barrier study was analyzed and compared to that obtained from acellular devices and additional control groups that contained epithelial or endothelial layers alone.

Results—Our microfluidic cell culture system provided a tightly controlled fluidic environment conducive to the proliferation and maintenance of JEG-3 trophoblasts and HUVECs on the ECM scaffold. Prolonged culture in this model produced confluent cellular monolayers on the intervening membrane that together formed the placental barrier. This *in vivo*-like microarchitecture was also critical for creating a physiologically relevant effective barrier to glucose transport. Quantitative investigation of barrier function was conducted by calculating permeability coefficients and metabolic rates in varying conditions of barrier structure. The rates of glucose transport and metabolism were consistent with previously reported *in vivo* observations.

Conclusion—The "Placenta-on-a-Chip" microdevice described herein provides new opportunities to simulate and analyze critical physiological responses of the placental barrier. This system may be used to address the major limitations of existing placenta model systems and serve to enable research platforms for reproductive biology and medicine.

Keywords

placental barrier; placenta *in vitro* model; organ-on-a-chip; microfluidics; glucose transfer

Introduction

The placenta is key to successful reproduction. Its most important function is the exchange of endogenous and exogenous substances, which enables adequate supply of oxygen and nutrients, excretion of fetal metabolic waste (1–6), and protection against potentially harmful agents, such as xenobiotics (7–11), bacteria (12–17), viruses (18–26), and parasites (26–32). Transfer of substances between the intervillous space and fetal capillaries takes place across a multilayered structure often called the "placental barrier," which is composed of trophoblasts, connective tissue, basal lamina, and the fetal endothelium (1–6, 33–37). The four major mechanisms responsible for this critical process are: 1) passive diffusion; 2) facilitated diffusion; 3) active transport; and 4) endocytosis/exocytosis (38–40). Moreover, biochemical and physical factors influence the dynamics of placental transfer, including

utero-placental and umbilical blood flow, barrier thickness, placental metabolism, concentration gradients, and transporter expression/activity in the placenta (41, 42).

Previous studies on placental transport have used a wide range of experimental systems including *in vivo* animal models (43–60), *ex vivo* placental perfusion systems (61–65), and *in vitro* cell cultures (10, 66–73). In some cases, placental transfer has been studied in humans for frequently used therapeutic agents such as antibiotics and hormones (7–10, 74–78). However, such studies are difficult to perform, time-consuming, and always carry the risk of exposure to the fetus. With the increasing availability of human tissue for laboratory studies, alternatives to animal models have been developed that rely on intact human placental tissue (79). Although these new types of model systems provide advantages in recapitulating human-relevant physiology, the lack of standardization in this strategy often leads to conflicting results due to lab-to-lab variability (79). Similarly, other *ex vivo* approaches, such as placental perfusion models (61–63,65, 79–84), have limited ability to dissect the process of placental transfer and to reveal mechanistic insights into its biological underpinnings at physiologically relevant length scales. Cell culture systems have been successfully used in improving the understanding of placental transfer and metabolism (66–69,72, 85–87). However, they largely fail to reconstitute the physiological structure and microenvironment that profoundly influence transport processes, raising major questions regarding their adequacy as an experimental platform in the study of this placental function (79).

Herein, we propose a new bioengineering approach to model placental transport that combines microfluidics and microfabrication technologies with the culture of placenta-derived human cells to recapitulate the organ-specific architecture and physiological microenvironment critical to placental barrier function. Specifically, we developed a “Placenta-on-a-Chip” microdevice that enabled compartmentalized perfusion co-culture of human trophoblasts (JEG-3) and human umbilical vein endothelial cells (HUVECs) on a thin extracellular matrix (ECM) membrane to create a physiological placental barrier *in vitro*. In this report, we employ novel microengineering techniques required for the fabrication of this biomimetic system, as well as prolonged maintenance of microfluidic co-culture in the microdevice. We also demonstrate the physiological function and relevance of this model by analyzing glucose transport across a microengineered placental barrier. This approach creates new opportunities to address major limitations of existing placenta models and holds great potential as a novel enabling platform for the study of placental barrier function.

Materials and Methods

Cell culture

JEG-3 (ATCC, Manassas, VA, USA) was selected among various trophoblasts cell lines (79). The cells were cultured in DMEM (Dulbecco’s Modified Eagle Medium, Gibco, Grand Island, NY) supplemented with 10% fetal bovine serum (FBS) and 1% penicillin/streptomycin. Cells with passages below 15 were used in microfluidic cell culture experiments.

Green fluorescent protein (GFP)-expressing HUVECs (Angio-Proteomie, Boston, MA) were cultured in EGM™-2 basal medium (Lonza, Walkersville, MD) supplemented with the EGM™-2 MV BulletKit (Lonza). Cells with passages below 10 were used in microfluidic cell culture experiments. Both cell lines were maintained at 37 °C in a humidified incubator under 5% CO_2 in air.

Device design and fabrication

To create the placenta-on-a-chip microdevice, two poly(-dimethylsiloxane) (PDMS) slabs containing microchannel features were bonded together with a vitrified collagen membrane sandwiched in between (Figure 1A). This design allowed for the independent control of fluid flows in the upper and lower channels, which correspond to the fetal capillary compartment and intervillous space, respectively (Figure 1B).

PDMS microchannels were generated using soft-lithography (88). Briefly, a negative photoresist (PR) (SU-8 2075, MicroChem Corp., Westborough, MA) was spin-coated on a clean silicon wafer (Taewon Scientific, Seoul, Republic of Korea) and baked first at 65 °C for 7 minutes and then at 95 °C for 40 minutes. Subsequently, the photoresist layer was brought in contact with a mask film containing channel patterns and exposed to ultraviolet (UV) light. Following this step, the wafer was baked again at 65 °C for 5 minutes and at 95 °C for 18 minutes before being placed in a developer solution to dissolve the unexposed photoresist. Finally, the wafer was thoroughly rinsed with copious amounts of the developer solution and isopropyl alcohol to generate a mold containing the positive relief of the desired microchannel patterns (Figure 2A).

For the fabrication of PDMS channels (Figure 2B), PDMS prepolymer was mixed with a curing agent at a weight ratio of 10:1 (prepolymer : curing agent) and placed in a vacuum chamber to remove trapped air. After degassing, the PDMS mixture was poured onto the channel mold and incubated at 65°C for 4 hours. When the PDMS mixture was fully cured, it was detached from the mold and cut into a desired shape and size to generate an upper PDMS slab engraved with a microchannel (Figure 2B). This replica molding process was repeated to produce a lower PDMS layer. The cross-sectional size of the microchannel in each layer was approximately 500 μm × 200 μm (width × height).

For the formation of the vitrified collagen membrane (Figure 2B), collagen type I (BD Biosciences, San Jose, CA) was mixed with distilled water and 10 × DMEM (Dulbecco's Modified Eagle Medium, Sigma–Aldrich Corp., St. Louis, MO) at a final concentration of 2.43 mg ml^{-1}. The pH of the solution was adjusted to 7.4 using 1N Sodium hydroxide (NaOH). The gel solution was gently dispensed on the central part of the lower microchannel and then incubated at 37 °C for 40 minutes for gelation. Subsequently, the collagen gel was dried overnight at room temperature to produce a vitrified collagen membrane that remained attached to the lower PDMS microchannel.

As the final step of device fabrication, the PDMS surfaces of the upper and lower channels were treated with plasma using a plasma cleaner (Harrick Plasma, Ithaca, NY, USA) and bonded together. During this step, care was taken to ensure the alignment of the upper and lower microchannels. Incubation of the bonded channels at 65 °C for 30 minutes produced a

permanently sealed microfluidic device that allowed for independent fluidic access to the upper and lower microchannels.

Microfluidic cell seeding and culture

Prior to cell seeding, silicon tubing (Tygon tube with an inner diameter of 1/32 inch) was inserted into the inlet and outlet ports of both channels to facilitate the handling of cells and fluids. The inlet tubing was used to connect the upper and lower microchannels to two separate reservoirs for cell culture media. The fully assembled device was sterilized by UV irradiation immediately before cell seeding.

To promote cell attachment and growth, the upper and lower surfaces of the vitrified membrane were coated with 40 μg ml^{-1} of fibronectin (BD Biosciences) and 1.5% gelatin (Sigma-Aldrich), respectively. Following ECM coating, trophoblasts (JEG-3 cells) (ATCC) suspended in a complete growth medium at 5×10^6 cells ml^{-1} were gently injected into the lower channel using a BD Falcon 1 mL syringe (BD Biosciences) and allowed to attach to the lower membrane surface (Figure 2C). The device remained inverted for the entire duration of this procedure. Once the trophoblasts established firm attachment, green fluorescent protein (GFP)-expressing HUVECs (Angio-Proteomie) were introduced into the upper microchannel and incubated for two hours to enable their adhesion to the upper side of the vitrified membrane (Figure 2C). For microfluidic culture, JEG-3 cells and HUVECs were perfused with their respective media using a syringe pump (Braintree Scientific, Inc., Braintree, MA) connected to the outlets that withdrew at a constant volumetric flow rate of 30 μl h^{-1}.

Monitoring and analysis of cell growth

Formation and structural integrity of the placental barrier in our co-culture model were assessed using confocal microscopy of the confluent monolayers of JEG-3 cells and GFP-HUVECs on the opposite sides of the membrane. For fluorescence imaging, JEG-3 cells were labeled with CellTracker™ Red CMTPX (Invitrogen, Life Technologies, Carlsbad, CA) prior to cell seeding. Fluorescence micrographs of the cells were acquired after 3 days of culture and the resultant confluences were analyzed using an image-processing algorithm developed using MATLAB® (Natick, MA).

Measurement of glucose transfer across the placental barrier

The cells in our microfluidic device were cultured for at least three days in order to ensure the maturation of the placental barrier. To recapitulate physiological gradients of glucose across the maternal-fetal interface, DMEM supplemented with a higher concentration (4.5 g ml^{-1}) of glucose was supplied to the lower trophoblast culture chamber, while EGM™-2 containing a lower glucose concentration (1.1 g ml^{-1}) was introduced into the upper endothelial channel. Continuous flow of the culture media was maintained at 30 μl h^{-1} for 68 hours, and perfused media were collected from the outlets of the upper and lower microchannels separately at the end of each experiment. The concentration of glucose in the collected samples was measured using a glucose analyzer (YSI Life Sciences, Yellow Springs, OH), and the results were analyzed in comparison to those obtained from the

following three control groups: i) an acellular model; ii) a mono-culture model with JEG-3 cells alone; and iii) a mono-culture model with HUVECs alone.

Analysis of glucose transfer—The rate of glucose transfer in our model was evaluated using a previously described method (89). Briefly, the percent rate of transfer (%TR) was calculated as follows:

$$\%\mathrm{TR}=\frac{\Delta Q_U}{\Delta Q_L}\times 100 \quad (1)$$

where ΔQ_U and ΔQ_L refer to the increasein glucose concentration in the upper and lower channels, respectively. Glucose permeability coefficients (GP) were calculated using the following equation,

$$\mathrm{GP}=\frac{\Delta Q}{\Delta t}\times\frac{1}{A\cdot C_L} \quad (2)$$

where ΔQ is the amount of glucose transferred to the upper channel, Δt is the time elapsed, A is the surface area of the placental barrier, and C_L is the glucose concentration in the lower channel. In our analysis, C_L was assumed to be constant due to flow-induced continuous replenishment of glucose in the lower channel. The glucose permeability coefficient of an unsupported cell monolayer ($\mathrm{GP_{UM}}$) (i.e., without the vitrified collagen membrane) was calculated using the equation derived by Utoguchi *et al*(90),

$$\mathrm{GP}_{\mathrm{UM}}=\left(\frac{1}{\mathrm{GP}_{\mathrm{SM}}}-\frac{1}{\mathrm{GP}_{\mathrm{CV}}}\right)^{-1} \quad (3)$$

where $\mathrm{GP_{SM}}$ and $\mathrm{GP_{CV}}$ refer to the glucose permeability coefficients of a cell monolayer ported by the membrane and the collagen vitrified membrane alone, respectively. Similarly, the glucose permeability coefficient of the bi-layer ($\mathrm{GP_{BL}}$) barrier consisting of JEG-3 and HUVEC monolayers was determined by the following equation,

$$\mathrm{GP}_{\mathrm{BL,derived}}=\left(\frac{1}{\mathrm{GP}_{\mathrm{JM}}}+\frac{1}{\mathrm{GP}_{\mathrm{CV}}}+\frac{1}{\mathrm{GP}_{\mathrm{HM}}}\right)^{-1} \quad (4)$$

where $\mathrm{GP_{JM}}$ and $\mathrm{GP_{HM}}$ are the permeability coefficients of unsupported JEG-3 and HUVEC monolayers. This $\mathrm{GP_{BL,derived}}$ refers to a theoretically derived glucose permeability coefficient of the barrier formed by physical superposition of JEG-3 and HUVEC monolayers and the vitrified collagen membrane without considering their functional interactions.

Statistical analysis—Experimental data were obtained from at least 6 independent experiments. Statistical significance was determined using ANOVA followed by Tukey's *post hoc* tests.

Results

Cell growth on the vitrified collagen membrane

Our microfluidic culture conditions provided an environment conducive to proliferation and maturation of JEG-3 cells and HUVECs in the co-culture model. As illustrated in the fluorescence micrographs of the cells in Figure 3, three days of perfusion culture in the device produced highly confluent monolayers of JEG-3 cells and HUVECs on either side of the membrane that resembled the microarchitecture of the placental barrier *in vivo*. Our imaging analysis revealed that the JEG-3 cells and HUVECs in our microdevice reached a confluency of 99.3% and 99.4%, respectively. Although the vitrified membrane underwent rapid rehydration upon injection of ECM coating solutions into the channels, it remained intact without undesirable structural deformation for the entire duration of culture and supported cell attachment and growth. We did not observe cross-contamination between the epithelial and endothelial populations due to cellular migration across the membrane.

Glucose transfer across the placental barrier

To evaluate the transport of glucose from the maternal to the fetal side in our model, we first measured changes in glucose concentration in the outflow collected from the upper (fetal) channel. The amount of glucose transferred to the fetal compartment was found to be the smallest in the co-culture model, illustrating the ability of the bi-layer microarchitecture to limit molecular transport across the barrier (Figure 4A). Glucose transfer was higher in the devices with JEG-3 cells or HUVECs alone, but the HUVECs monoculture model exhibited a greater magnitude of concentration increase. This observation suggests that the trophoblast epithelium serves as the main barrier to glucose transport. The absence of cellular components in the acellular model resulted in substantially increased transfer across the membrane and concomitant elevation of glucose concentration in the fetal endothelial compartment.

To examine more closely the placental barrier function in our model, we also evaluated reduction of the glucose concentration in the lower maternal compartment (Figure 4B). Interestingly, the magnitude of decrease was the largest whenJEG-3 cells were cultured alone, and our co-culture configuration led to a greater reduction in glucose concentration compared to the HUVECs monoculture and acellular devices. It was also noted that the endothelial layer in the HUVECs monoculture model induced a greater depletion of glucose in the lower channel. The differences in glucose concentration in the upper and lower channels imply that transport of glucose across the barrier in this model is governed by mechanisms other than concentration gradient-induced passive diffusion and that the cells serve as a critical determinant of glucose transfer. Moreover, glucose transporters expressed by placental cells may contribute to the mechanisms responsible for glucose transfer in our device.

Quantitative analysis of glucose transfer

Glucose passed through the vitrified collagen membrane without much hindrance, as shown by the relatively high transfer rates (67.8–99.5%) (Figure 5). However, when cells were incorporated into the device, the transfer rate decreased substantially. The HUVECs monoculture model yielded a transfer rate of 45.5–93%, and this was further reduced to 17.3–39.1% with the addition of trophoblasts, confirming their predominant role in placental barrier function.

Evaluation of glucose permeability coefficients (GPs) showed that the GP for a monolayer of HUVECs was significantly greater than that of JEG-3 cells, indicating that the endothelial cells cultured in our model were more permeable to glucose than trophoblasts (Figure 6). The $GP_{BL,derived}$ calculated using equation (4) was 1.02×10^{-4}cm s^{-1}, and this value was in the range of experimentally obtained GPs for the bi-layer (BL) model. The $GP_{BL,derived}$ was evaluated without considering the association of the epithelial barrier with the endothelium; the results suggest that glucose transfer may not be affected by functional interactions between trophoblasts and endothelial cells.

Discussion

We developed a “Placenta-on-a-Chip” device inhabited by living human cells which recapitulate the critical fetal-maternal interface in the villous tree of the human placenta. Trophoblasts and HUVECs were co-cultured in a compartmentalized three-dimensional PDMS microsystem consisting of the upper and lower cell culture chambers separated by a thin vitrified collagen membrane. The resultant bi-layer tissue resembled a physiological placental barrier, which is often challenging to generate using standard two-dimensional cell culture methods. We also demonstrated that continuous perfusion of the cells in our microfluidic device supported cell growth and long-term viability.

We analyzed glucose transfer characteristics across the microengineered placental barrier. Glucose was chosen as a model molecule due to i) its importance in normal pregnancy (40, 91–93), gestational diabetes (40, 93–97), and overt diabetes (93, 98), and ii) its permeability across the placental barrier in spite of placental metabolism. The transfer rates measured in our model ranged from 22.6% to 33.9%, indicating metabolic consumption (66.1~77.4%). These results are consistent with previously reported placental metabolic rates in the lamb (99). However, direct comparison was not possible due to a paucity of such data in the literature. Based on these results, we conclude that our model mimics not only structural characteristics of the human placental barrier but also some aspects of physiology.

Despite its capabilities and advantages, our system has limitations. From the perspective of model development, although our microfluidic culture system provides a greater physiological cell culture environment than conventional static cultures, the levels of shear stress generated in our model are substantially lower than those in fetal capillaries. This is mainly due to the large size of the cell culture chambers and could be overcome simply by reducing the dimensions of the fetal compartment and/or increasing the rate of fluid flow on the fetal side. We employed the JEG-3 cell line and HUVECs to represent trophoblast and

endothelial cells, respectively. Future studies using primary human trophoblasts (100) and fetal capillary endothelial cells need to be performed.

Our placenta-on-a-chip model has potential to serve as a low-cost experimental platform with a broad range of applications. For example, the capabilities afforded by this microsystem provide new opportunities to quantitatively and mechanistically investigate placental transfer of various substances under varying conditions and to eventually improve our fundamental understanding of complex human placental physiology. This biomimetic model may also enable the quantitative analysis of placental transport of small molecules and biologics for the development and screening of new therapeutic modalities. Moreover, the microengineering approach demonstrated in this study could be leveraged to recapitulate key pathological features of different placental disorders to develop new types of in vitro human disease models. As exemplified by the recent launching of the Human Placenta Project by NICHD/NIH (101), there has been a growing interest in the application of microengineered physiological systems to the study of placental biology. Our placenta-on-a-chip model represents exciting progress in this area and lays the groundwork for future studies aiming to explore the potential of organs-on-chips technology for reproductive biology and medicine.

Acknowledgments

This work was supported, in part, by the Perinatology Research Branch, Division of Intramural Research, Eunice Kennedy Shriver National Institute of Child Health and Human Development, National Institutes of Health, U.S. Department of Health and Human Services (NICHD/NIH/DHHS) and, in part, with Federal funds from NICHD/NIH/DHHS under Contract No. HHSN275201300006C, and by the Seoul National University Bundang Hospital Research Fund (Grant No. 03-2013-001) and the National Research Foundation of Korea (2012M3A7B4035286 and 2013R1A2A2A04013379). We also acknowledge support from the National Medical Center and Asan Medical Center in Seoul, Republic of Korea. D. H. is a recipient of the NIH Director's New Innovator Award (1DP2HL127720-01).

References

1. Fox H. Pathology of the placenta. Clin Obstetrics Gynaecol. 1986; 13:501–519.
2. Kraus, FT., Redline, RW., Gersell, DJ., Nelson, RN., Dicke, JM. Placental pathology. First. Washington, DC: American Registry of Pathology; 2004.
3. Fox, H., Sebire, NJ. Pathology of the placenta. Third. Philadelphia, PA: Elsevier; 2007.
4. Kay, HH., Nelson, MD., Wang, Y. The placenta from development to disease. First. New Jersey: Blackwell; 2011.
5. Benirschke, K., Burton, GJ., Baergen, RN. Pathology of the human placenta. Sixth. Berlin: Springer; 2012.
6. Burton GJ, Fowden AL. Review: The placenta and developmental programming: balancing fetal nutrient demands with maternal resource allocation. Placenta. 2012; 33:S23–S27. [PubMed: 22154688]
7. Hakkola J, Pelkonen O, Pasanen M, Raunio H. Xenobiotic-metabolizing cytochrome P450 enzymes in the human feto-placental unit: role in intrauterine toxicity. Crit Rev Toxicol. 1998; 28:35–72. [PubMed: 9493761]
8. Myllynen P, Pasanen M, Vahakangas K. The fate and effects of xenobiotics in human placenta. Expert Opin Drug Metab Toxicol. 2007; 3:331–346. [PubMed: 17539742]
9. Polachek H, Holcberg G, Polachek J, Rubin M, Feinshtein V, Sheiner E, et al. Carrier-mediated uptake of Levofloxacin by BeWo cells, a human trophoblast cell line. Arch Gynecol Obstet. 2010; 281:833–838. [PubMed: 19629508]

10. Prouillac C, Lecoeur S. The role of the placenta in fetal exposure to xenobiotics: importance of membrane transporters and human models for transfer studies. Drug Metab Dispos. 2010; 38:1623–1635. [PubMed: 20606001]
11. Grafmuller S, Manser P, Krug HF, Wick P, von Mandach U. Determination of the transport rate of xenobiotics and nanomaterials across the placenta using the ex vivo human placental perfusion model. J Vis Exp. 2013; 76:e50401.
12. Benirschke K. Syphilis--the placenta and the fetus. Am J Dis Child. 1974; 128:142–143. [PubMed: 4854595]
13. Barber EM, Fazzari M, Pollard JW. Th1 cytokines are essential for placental immunity to *Listeria monocytogenes*. Infect Immun. 2005; 73:6322–6331. [PubMed: 16177303]
14. Lecuit M. Understanding how *Listeria monocytogenes* targets and crosses host barriers. Clin Microbiol Infect. 2005; 11:430–436. [PubMed: 15882192]
15. Seveau S, Pizarro-Cerda J, Cossart P. Molecular mechanisms exploited by *Listeria monocytogenes* during host cell invasion. Microbes Infect. 2007; 9:1167–1175. [PubMed: 17761447]
16. Qi Z, Zhao H, Zhang Q, Bi Y, Ren L, Zhang X, et al. Acquisition of maternal antibodies both from the placenta and by lactation protects mouse offspring from *Yersinia pestis* challenge. Clin Vaccine Immunol. 2012; 19:1746–1750. [PubMed: 22933398]
17. Zeldovich VB, Clausen CH, Bradford E, et al. Placental syncytium forms a biophysical barrier against pathogen invasion. PLoS Pathog. 2013; 9:e1003821. [PubMed: 24348256]
18. Burton GJ, Watson AL. The structure of the human placenta: implications for initiating and defending against virus infections. Rev Med Virol. 1997; 7:219–28. [PubMed: 10398486]
19. Halwachs-Baumann G. The congenital cytomegalovirus infection: virus-host interaction for defense and transmission. Curr Pharm Biotechnol. 2006; 7:303–12. [PubMed: 16918406]
20. Koga K, Cardenas I, Aldo P, et al. Activation of TLR3 in the trophoblast is associated with preterm delivery. Am J Reprod Immunol. 2009; 61:196–212. [PubMed: 19239422]
21. Cardenas I, Means RE, Aldo P, et al. Viral infection of the placenta leads to fetal inflammation and sensitization to bacterial products predisposing to preterm labor. J Immunol. 2010; 185:1248–57. [PubMed: 20554966]
22. Aldo PB, Mulla MJ, Romero R, et al. Viral ssRNA induces first trimester trophoblast apoptosis through an inflammatory mechanism. Am J Reprod Immunol. 2010; 64:27–37. [PubMed: 20175771]
23. Moodley S, Bobat R. Expression of HLA-G1 at the placental interface of HIV-1 infected pregnant women and vertical transmission of HIV. Placenta. 2011; 32:778–82. [PubMed: 21816469]
24. Cardenas I, Mor G, Aldo P, et al. Placental viral infection sensitizes to endotoxin-induced pre-term labor: a double hit hypothesis. Am J Reprod Immunol. 2011; 65:110–17. [PubMed: 20712808]
25. Pereira L, Petitt M, Tabata T. Cytomegalovirus infection and antibody protection of the developing placenta. Clin Infect Dis. 2013; 57:S174–7. [PubMed: 24257421]
26. Moro L, Bardaji A, Nhampossa T, et al. Malaria and HIV infection in mozambican pregnant women are associated with reduced transfer of antimalarial antibodies to their newborns. J Infect Dis. 2015; 211:1004–14. [PubMed: 25271267]
27. Staalsoe T, Shulman CE, Bulmer JN, et al. Variant surface antigenspecific IgG and protection against clinical consequences of pregnancy-associated Plasmodium falciparum malaria. Lancet. 2004; 24(363):283–9.
28. Duffy PE. Plasmodium in the placenta: parasites, parity, protection, prevention and possibly preeclampsia. Parasitology. 2007; 134:1877–81. [PubMed: 17958923]
29. Castillo C, Lopez-Munoz R, Duaso J, et al. Role of matrix metalloproteinases 2 and 9 in ex vivo Trypanosoma cruzi infection of human placental chorionic villi. Placenta. 2012; 33:991–7. [PubMed: 23107342]
30. Diaz-Lujan C, Triquell MF, Schijman A, et al. Differential susceptibility of isolated human trophoblasts to infection by Trypanosoma cruzi. Placenta. 2012; 33:264–70. [PubMed: 22296856]
31. Bedu-Addo G, Meese S, Mockenhaupt FP. An ATP2B4 polymorphism protects against malaria in pregnancy. J Infect Dis. 2013; 207:1600–3. [PubMed: 23444010]

32. Liempi A, Castillo C, Duaso J, et al. Trypanosoma cruzi induces trophoblast differentiation: a potential local antiparasitic mechanism of the human placenta? Placenta. 2014; 35:1035–42. [PubMed: 25315217]
33. Nagashige M, Ushigome F, Koyabu N, et al. Basal membrane localization of MRP1 in human placental trophoblast. Placenta. 2003; 24:951–8. [PubMed: 14580377]
34. Myren M, Mose T, Mathiesen L, Knudsen LE. The human placenta – an alternative for studying foetal exposure. Toxicol In Vitro. 2007; 21:1332–40. [PubMed: 17624715]
35. Pijnenborg, R., Brosen, I., Romero, R. Placenta bed disorders. Cambridge, UK: Cambridge University Press; 2010.
36. Levkovitz R, Zaretsky U, Gordon Z, et al. In vitro simulation of placental transport: part I. Biological model of the placental barrier. Placenta. 2013; 34:699–707. [PubMed: 23764139]
37. Levkovitz R, Zaretsky U, Jaffa AJ, et al. In vitro simulation of placental transport: part II. Glucose transfer across the placental barrier model. Placenta. 2013; 34:708–15. [PubMed: 23764138]
38. Knipp GT, Audus KL, Soares MJ. Nutrient transport across the placenta. Adv Drug Deliv Rev. 1999; 38:41–58. [PubMed: 10837745]
39. Sibley CP, Brownbill P, Dilworth M, Glazier JD. Review: adaptation in placental nutrient supply to meet fetal growth demand: implications for programming. Placenta. 2010; 31:S70–4. [PubMed: 20060581]
40. Lager S, Powell TL. Regulation of nutrient transport across the placenta. J Preg. 2012; 2012:179827.
41. Carter AM. Evolution of factors affecting placental oxygen transfer. Placenta. 2009; 30A:S19–25.
42. Gaccioli F, Lager S, Powell TL, Jansson T. Placental transport in response to altered maternal nutrition. J Dev Orig Health Dis. 2013; 4:101–15. [PubMed: 25054676]
43. Rosso P. Maternal-fetal exchange during protein malnutrition in the rat. Placental transfer of alpha-amino isobutyric acid. J Nutr. 1977; 107:2002–5. [PubMed: 908958]
44. Rosso P. Maternal-fetal exchange during protein malnutrition in the rat. Placental transfer of glucose and a nonmetabolizable glucose analog. J Nutr. 1977; 107:20006–10. [PubMed: 908957]
45. Saintonge J, Rosso P. Placental blood flow and transfer of nutrient analogs in large, average, and small guinea pig littermates. Pediatr Res. 1981; 15:152–6. [PubMed: 7254941]
46. Ahokas RA, Lahaye EB, Anderson GD, Lipshitz J. Effect of maternal dietary restriction on fetal growth and placental transfer of alpha-amino isobutyric acid in rats. J Nutr. 1981; 111:2052–8. [PubMed: 7310531]
47. Jansson T, Persson E. Placental transfer of glucose and amino acids in intrauterine growth retardation: studies with substrate analogs in the awake guinea pig. Pediatr Res. 1990; 28:203–8. [PubMed: 2235115]
48. Varma DR, Ramakrishnan R. Effects of protein-calorie malnutrition on transplacental kinetics of aminoisobutyric acid in rats. Placenta. 1991; 12:277–84. [PubMed: 1754576]
49. Dwyer CM, Madgwick AJ, Crook AR, Stickland NC. The effect of maternal undernutrition on the growth and development of the guinea pig placenta. J Dev Physiol. 1992; 18:295–302. [PubMed: 1307381]
50. Malandro MS, Beveridge MJ, Kilberg MS, Novak DA. Effect of low-protein diet-induced intrauterine growth retardation on rat placental amino acid transport. Am J Physiol. 1996; 271:C295–303. [PubMed: 8760058]
51. Glazier JD, Sibley CP, Carter AM. Effect of fetal growth restriction on system A amino acid transporter activity in the maternal facing plasma membrane of rat syncytiotrophoblast. Pediatr Res. 1996; 40:325–9. [PubMed: 8827785]
52. Reid GJ, Lane RH, Flozak AS, Simmons RA. Placental expression of glucose transporter proteins 1 and 3 in growth-restricted fetal rats. Am J Obstet Gynecol. 1999; 180:1017–23. [PubMed: 10203672]
53. Lesage J, Hahn D, Leonhardt M, et al. Maternal undernutrition during late gestation-induced intrauterine growth restriction in the rat is associated with impaired placental GLUT3 expression, but does not correlate with endogenous corticosterone levels. J Endocrinol. 2002; 174:37–43. [PubMed: 12098661]

54. Jansson N, Pettersson J, Haafiz A, et al. Down-regulation of placental transport of amino acids precedes the development of intrauterine growth restriction in rats fed a low protein diet. J Physiol. 2006; 576:935–46. [PubMed: 16916910]
55. Schlabritz-Loutsevitch N, Ballesteros B, Dudley C, et al. Moderate maternal nutrient restriction, but not glucocorticoid administration, leads to placental morphological changes in the baboon (Papio sp.). Placenta. 2007; 28:783–93. [PubMed: 17382997]
56. Coan PM, Angiolini E, Sandovici I, et al. Adaptations in placental nutrient transfer capacity to meet fetal growth demands depend on placental size in mice. J Physiol. 2008; 586:4567–76. [PubMed: 18653658]
57. Barry JS, Rozance PJ, Anthony RV. An animal model of placental insufficiency-induced intrauterine growth restriction. Semin Perinatol. 2008; 32:225–30. [PubMed: 18482626]
58. Coan PM, Vaughan OR, Sekita Y, et al. Adaptations in placental phenotype support fetal growth during undernutrition of pregnant mice. J Physiol. 2010; 588:527–38. [PubMed: 19948659]
59. Sferruzzi-Perri AN, Vaughan OR, Coan PM, et al. Placental specific Igf2 deficiency alters developmental adaptations to undernutrition in mice. Endocrinology. 2011; 152:3202–12. [PubMed: 21673101]
60. Belkacemi L, Jelks A, Chen CH, et al. Altered placental development in undernourished rats: role of maternal glucocorticoids. Reprod Biol Endocrinol. 2011; 9:105–15. [PubMed: 21806804]
61. Schneider H, Panigel M, Dancis J. Transfer across the perfused human placenta of antipyrine, sodium and leucine. Am J Obstet Gynecol. 1972; 114:822–8. [PubMed: 4676572]
62. Polliotti BM, Holmes R, Cornish JD, et al. Long-term dual perfusion of isolated human placental lobules with improved oxygenation for infectious diseases research. Placenta. 1996; 17:57–68. [PubMed: 8710814]
63. Heikkila A, Myllynen P, Keski-Nisula L, et al. Gene transfer to human placenta ex vivo: a novel application of dual perfusion of human placental cotyledon. Am J Obstet Gynecol. 2002; 186:1046–51. [PubMed: 12015535]
64. Fokina VM, Patrikeeva SL, Zharikova OL, et al. Transplacental transfer and metabolism of buprenorphine in preterm human placenta. Am J Perinatol. 2011; 28:25–32. [PubMed: 20607647]
65. Woo CS, Partanen H, Myllynen P, et al. Fate of the teratogenic and carcinogenic ochratoxin A in human perfused placenta. Toxicol Lett. 2012; 208:92–9. [PubMed: 22037670]
66. Pattillo RA, Gey GO. The establishment of a cell line of human hormone-synthesizing trophoblastic cells in vitro. Cancer Res. 1968; 28:1231–6. [PubMed: 4299001]
67. Pattillo RA, Gey GO, Delfs E, et al. The hormone synthesizing trophoblastic cell in vitro: a model for cancer research and placental hormone synthesis. Ann N Y Acad Sci. 1971; 172:288–98. [PubMed: 5289994]
68. Kohler PO, Bridson WE. Isolation of hormone-producing clonal lines of human choriocarcinoma. J Clin Endocrinol Metab. 1971; 32:683–7. [PubMed: 5103722]
69. Azizkhan JC, Speeg KV Jr, Stromberg K, Goode D. Stimulation of human chorionic gonadotropin by JAr line choriocarcinoma after inhibition of DNA synthesis. Cancer Res. 1979; 39:1952–9. [PubMed: 156064]
70. Wice B, Menton D, Geuze H, Schwartz AL. Modulators of cyclic AMP metabolism induce syncytiotrophoblast formation in vitro. Exp Cell Res. 1990; 186:306–16. [PubMed: 2153559]
71. Miller RK, Genbacev O, Turner MA, et al. Human placental explants in culture: approaches and assessments. Placenta. 2005; 26:439–48. [PubMed: 15950058]
72. Wolfe MW. Culture and transfection of human choriocarcinoma cells. Methods Mol Med. 2006; 121:229–39. [PubMed: 16251747]
73. Orendi K, Kivity V, Sammar M, et al. Placental and trophoblastic in vitro models to study preventive and therapeutic agents for preeclampsia. Placenta. 2011; 32:S49–54. [PubMed: 21257083]
74. Pacifici GM, Nottoli R. Placental transfer of drugs administered to the mother. Clin Pharmacokinet. 1995; 28:235–69. [PubMed: 7758253]
75. Ushigome F, Takanaga H, Matsuo H, et al. Human placental transport of vinblastine, vincristine, digoxin and progesterone: contribution of P-glycoprotein. Eur J Pharmacol. 2000; 408:1–10. [PubMed: 11070177]

76. Syme MR, Paxton JW, Keelan JA. Drug transfer and metabolism by the human placenta. Clin Pharmacokinet. 2004; 43:487–514. [PubMed: 15170365]
77. Evseenko D, Paxton JW, Keelan JA. Active transport across the human placenta: impact on drug efficacy and toxicity. Expert Opin Drug Metab Toxicol. 2006; 2:51–69. [PubMed: 16863468]
78. Giaginis C, Tsantili-Kakoulidou A, Theocharis S. Assessing drug transport across the human placental barrier: from in vivo and in vitro measurements to the ex vivo perfusion method and in silico techniques. Curr Pharm Biotechnol. 2011; 12:804–13. [PubMed: 21480826]
79. Myllynen P, Vahakangas K. Placental transfer and metabolism: an overview of the experimental models utilizing human placental tissue. Toxicol In Vitro. 2013; 27:507–12. [PubMed: 22960472]
80. Nanovskaya TN, Nekhayeva IA, Patrikeeva SL, et al. Transfer of metformin across the dually perfused human placental lobule. Am J Obstet Gynecol. 2006; 195:1081–5. [PubMed: 16824464]
81. Nanovskaya TN, Nekhayeva IA, Hankins GD, Ahmed MS. Transfer of methadone across the dually perfused preterm human placental lobule. Am J Obstet Gynecol. 2008; 198:126 e1–4. [PubMed: 18166326]
82. Ceccaldi PF, Ferreira C, Gavard L, et al. Placental transfer of enfuvirtide in the ex vivo human placenta perfusion model. Am J Obstet Gynecol. 2008; 198:433 e1–2. [PubMed: 18241815]
83. Smith JA, Gaikwad A, Mosley S, et al. Utilization of an ex vivo human placental perfusion model to predict potential fetal exposure to carboplatin during pregnancy. Am J Obstet Gynecol. 2014; 210:275 e1–9. [PubMed: 24333234]
84. Mandelbrot L, Duro D, Belissa E, Peytavin G. Placental transfer of rilpivirine in an ex vivo human cotyledon perfusion model. Antimicrob Agents Chemother. 2015; 59:2901–3. [PubMed: 25691637]
85. Liu F, Soares MJ, Audus KL. Permeability properties of monolayers of the human trophoblast cell line BeWo. Am J Physiol. 1997; 273:C1596–604. [PubMed: 9374645]
86. Ampasavate C, Chandorkar GA, Vande Velde DG, et al. Transport and metabolism of opioid peptides across BeWo cells, an in vitro model of the placental barrier. Int J Pharm. 2002; 233:85–98. [PubMed: 11897413]
87. Tobin KA, Johnsen GM, Staff AC, Duttaroy AK. Long-chain polyunsaturated fatty acid transport across human placental choriocarcinoma (BeWo) cells. Placenta. 2009; 30:41–7. [PubMed: 19010540]
88. Xia Y, Whitesides GM. Soft lithography. Annu Rev Mater Sci. 1998; 28:153–84.
89. Vinot C, Gavard L, Treluyer JM, et al. Placental transfer of maraviroc in an ex vivo human cotyledon perfusion model and influence of ABC transporter expression. Antimicrob Agents Chemother. 2013; 57:1415–20. [PubMed: 23295922]
90. Utoguchi N, Magnusson M, Audus KL. Carrier-mediated transport of monocarboxylic acids in BeWo cell monolayers as a model of the human trophoblast. J Pharm Sci. 1999; 88:1288–92. [PubMed: 10585224]
91. Bax BE, Bloxam DL. Energy metabolism and glycolysis in human placental trophoblast cells during differentiation. Biochim Biophys Acta. 1997; 1319:283–92. [PubMed: 9131049]
92. Hay WW Jr. Placental-fetal glucose exchange and fetal glucose metabolism. Trans Am Clin Climatol Assoc. 2006; 117:321–39. (discussion 339–40). [PubMed: 18528484]
93. Brett KE, Ferraro ZM, Yockell-Lelievre J, et al. Maternal-fetal nutrient transport in pregnancy pathologies: the role of the placenta. Int J Mol Sci. 2014; 15:16153–85. [PubMed: 25222554]
94. Gaither K, Quraishi AN, Illsley NP. Diabetes alters the expression and activity of the human placental GLUT1 glucose transporter. J Clin Endocrinol Metab. 1999; 84:695–701. [PubMed: 10022440]
95. Jansson T, Ekstrand Y, Wennergren M, Powell TL. Placental glucose transport in gestational diabetes mellitus. Am J Obstet Gynecol. 2001; 184:111–16. [PubMed: 11174489]
96. Colomiere M, Permezel M, Riley C, et al. Defective insulin signaling in placenta from pregnancies complicated by gestational diabetes mellitus. Eur J Endocrinol. 2009; 160:567–78. [PubMed: 19179458]
97. Bibee KP, Illsley NP, Moley KH. Asymmetric syncytial expression of GLUT9 splice variants in human term placenta and alterations in diabetic pregnancies. Reprod Sci. 2011; 18:20–7. [PubMed: 20926839]

98. Jansson T, Wennergren M, Powell TL. Placental glucose transport and GLUT 1 expression in insulin-dependent diabetes. Am J Obstet Gynecol. 1999; 180:163–8. [PubMed: 9914598]

99. Simmons M, Battaglia F, Meschia G. Placental transfer of glucose. J Dev Physiol. 1979; 1:227–43. [PubMed: 551112]

100. Kliman HJ, Nestler JE, Sermasi E, et al. Purification, characterization, and in vitro differentiation of cytotrophoblasts from human term placentae. Endocrinology. 1986; 118:1567–82. [PubMed: 3512258]

101. NICHD. [last accessed 20 Feb 2015] The Human Placenta Project 2015. Available from: http://www.nichd.nih.gov/research/HPP/Pages/default.aspx

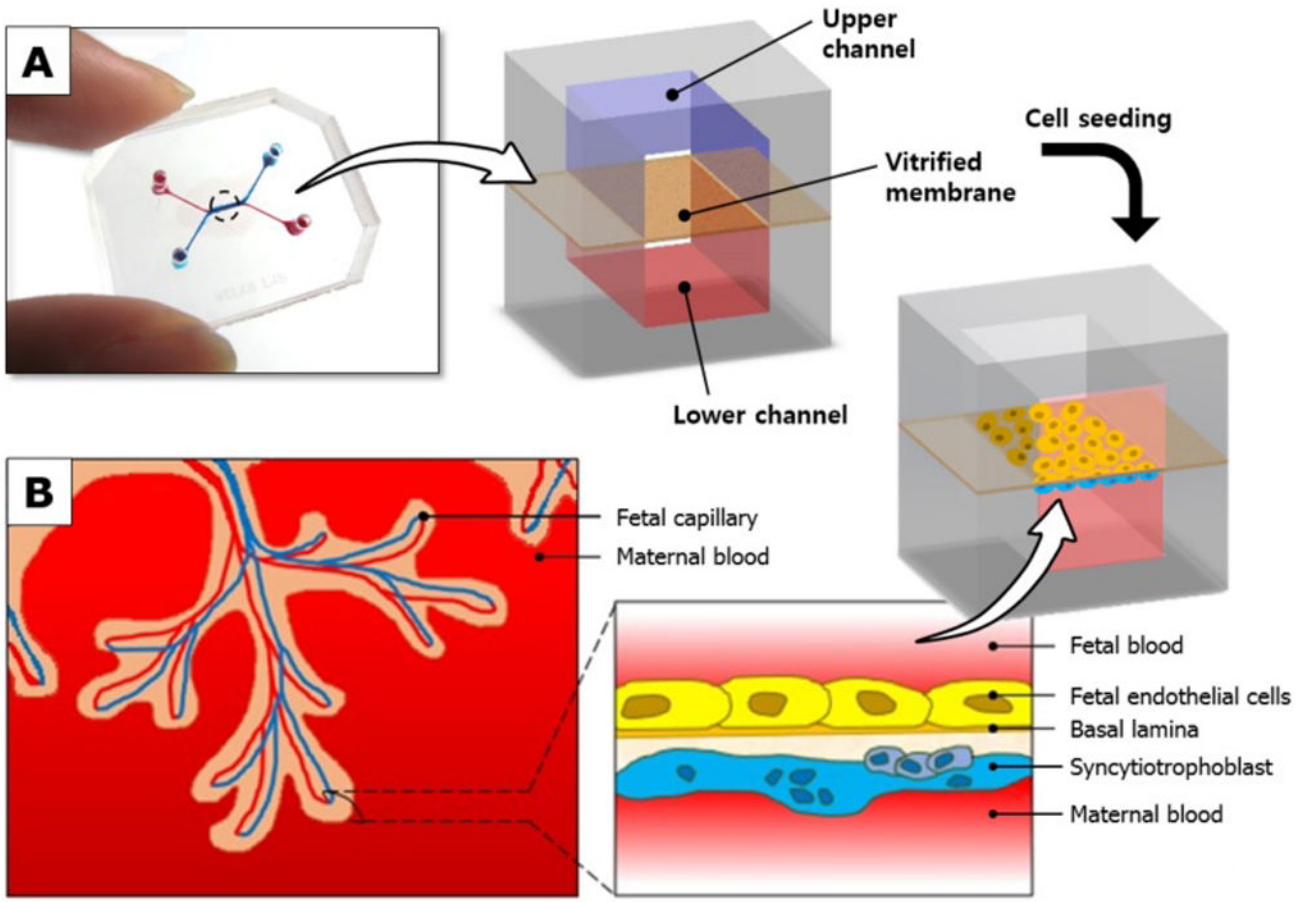

Figure 1.

A placenta-on-a-chip microdevice: A) The microengineered device is composed of the upper (blue) and lower (red) PDMS chambers separated by a vitrified collagen membrane. B) Endothelial cells and trophoblasts are co-cultured in close apposition on the opposite sides of the intervening membrane to form a microengineered placental barrier in the placenta-on-a-chip device.

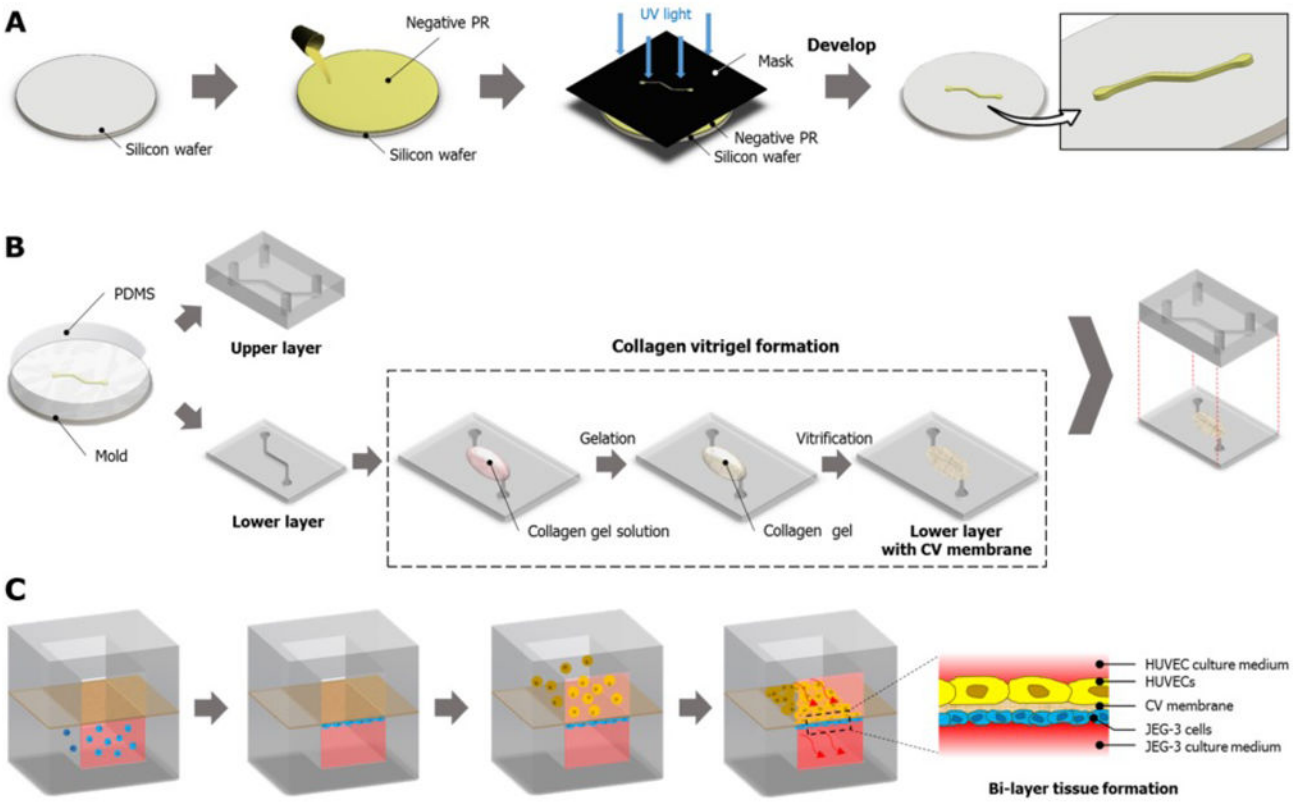

Figure 2.

Fabrication of the placenta-on-a-chip: A) Production of a microchannel master using photolithography. B) Soft lithography-based replica molding of PDMS microchannels and the formation of the vitrified collagen membrane. The upper PDMS slab is permanently bonded to the lower slab containing a microchannel covered with the vitrified membrane. C) Sequential seeding of JEG-3 cells and HUVECS in the multilayered microfluidic device.

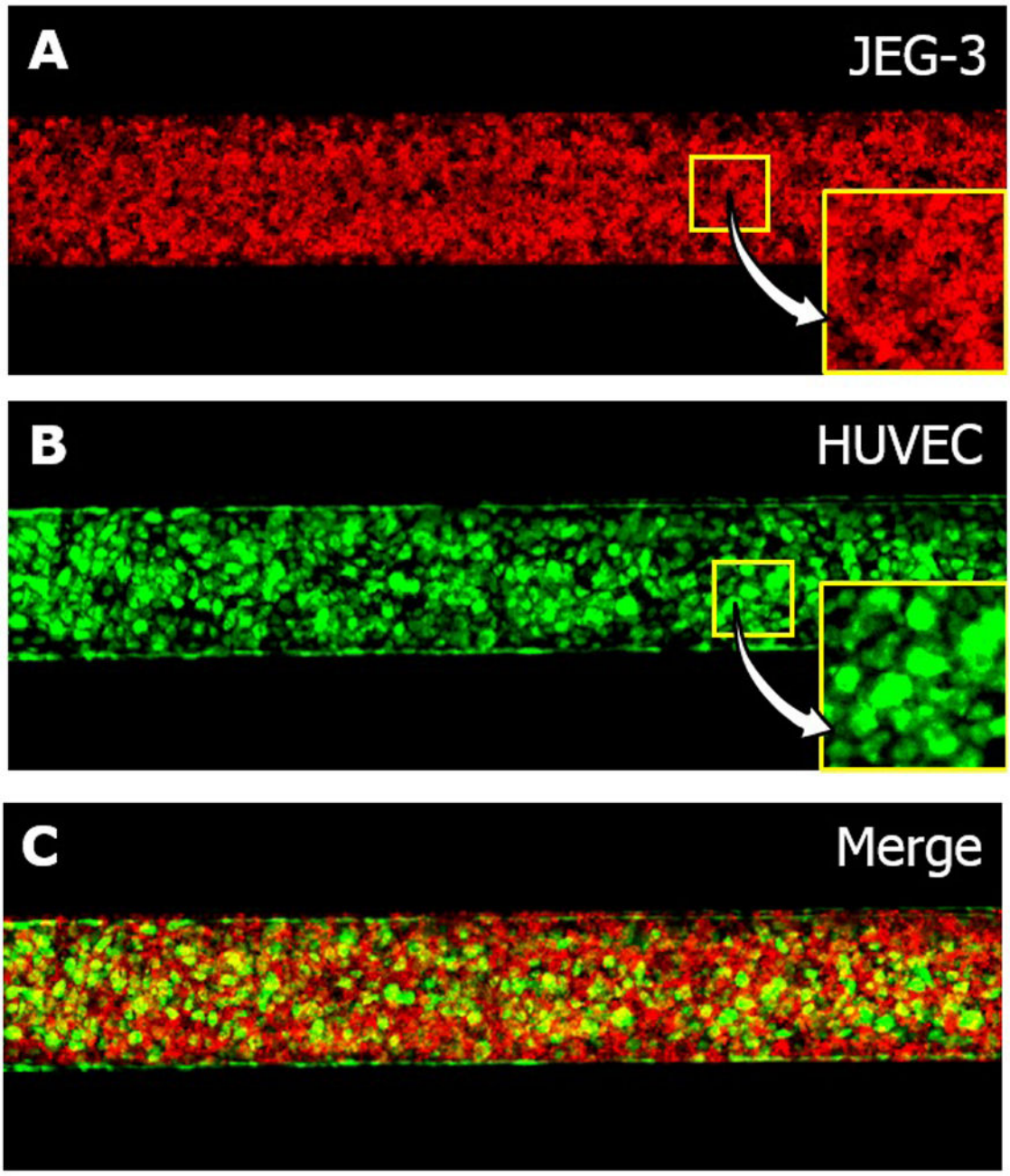

Figure 3.

A microengineered placental barrier: fluorescence micrographs of A) JEG-3 cells (red) and B) HUVECs (green) grown on the lower and upper membrane surfaces, respectively. C) A merge of A and B.

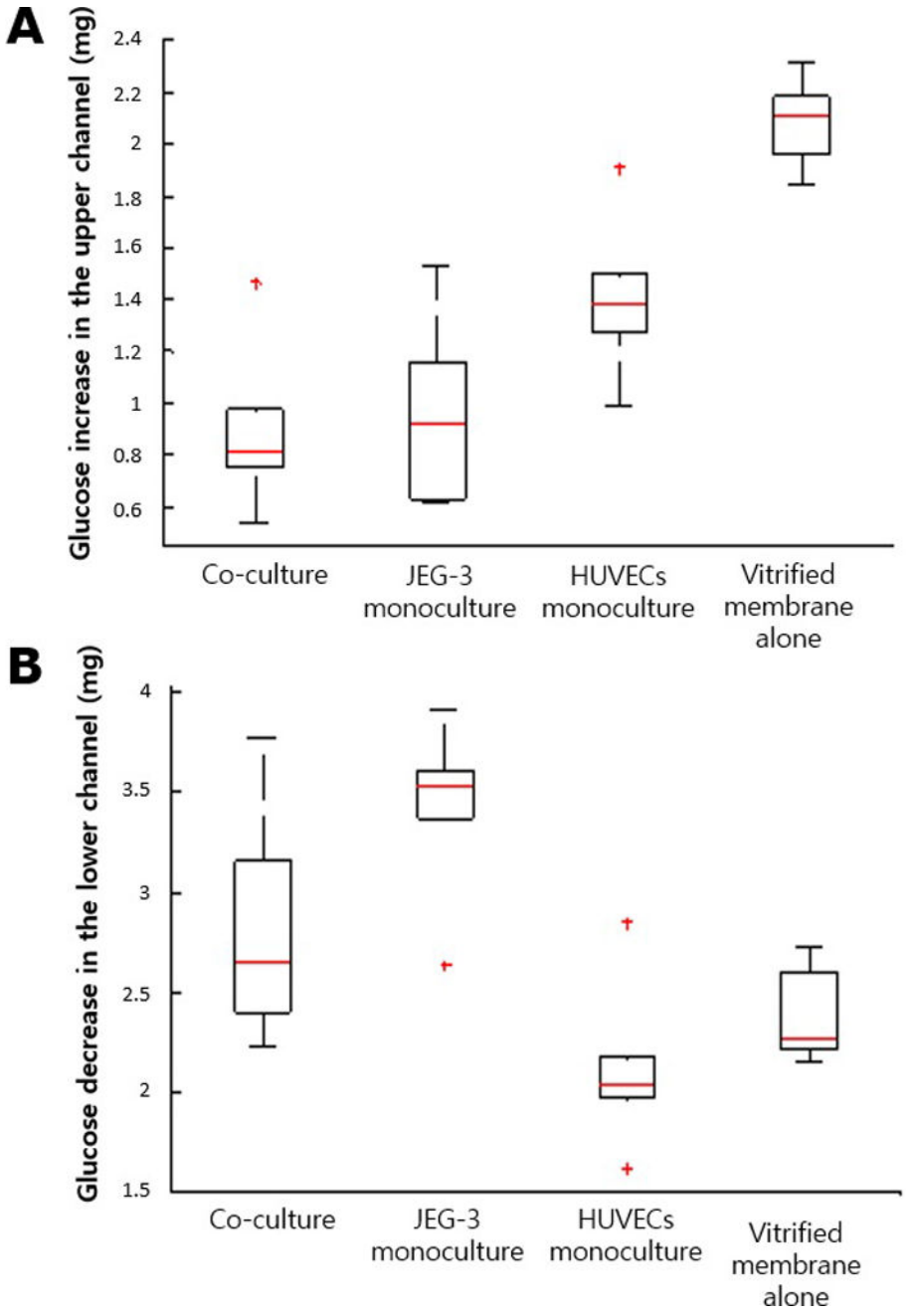

Figure 4.

Changes in the amounts of glucose: A) Glucose increases in the fetal compartment; B) Reduction in glucose concentration in the maternal chamber. Boxes denote the interquartile range, with the red horizontal line representing the median. Whiskers extend from the box to the extreme values unless there were outliers (+ red signs).

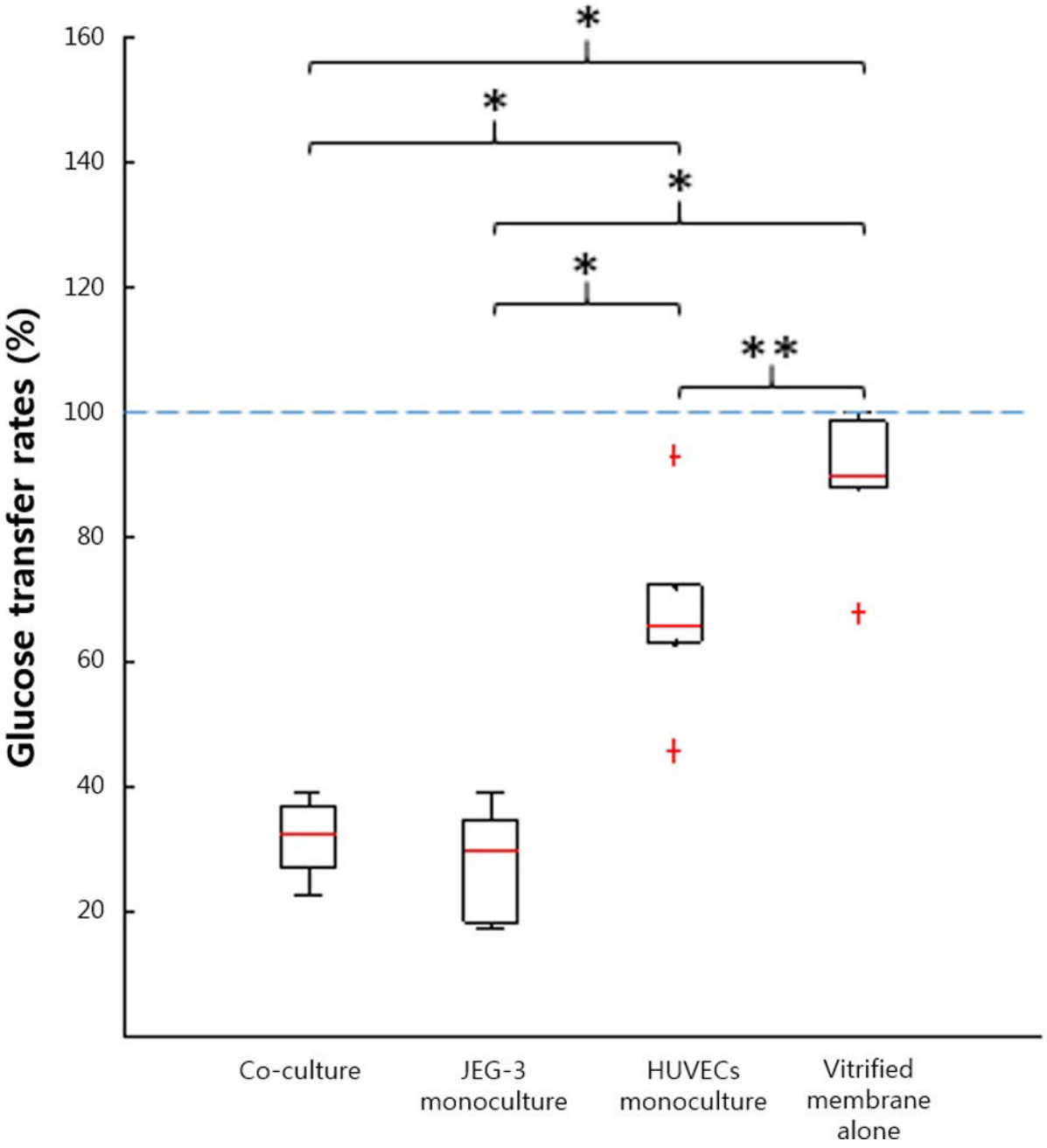

Figure 5.
Glucose transfer rates (%). * and ** represent P<0.01 and P<0.05, respectively.

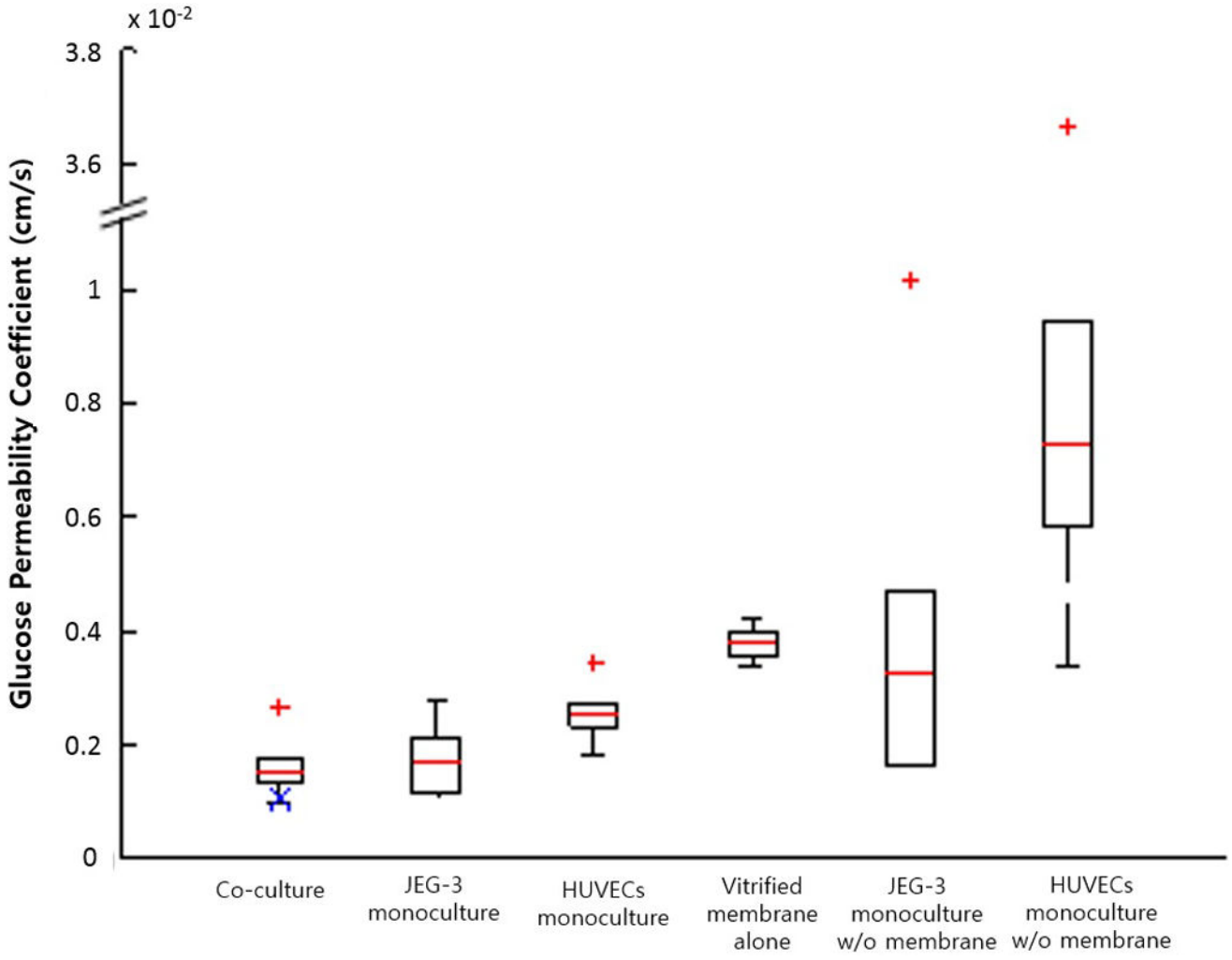

Figure 6.

Glucose permeability coefficients. $GP_{BL,derived}$ calculated using equation (4) is marked with a blue X in the co-culture group.